ADVANCED ENERGY MATERIALS
www.advenergymat.de

The Operation Dependence of $C - N$ Fatigue for Lithium-Ion Batteries

*Chunguang Chen, Qingrong Zou, Jici Wen, Jin Liu, Peter H. L. Notten, and Yujie Wei**

Lithium-ion batteries (LIBs) fatigue in repeated service, and their cycle-life, in resemblance to most materials subject to cyclic loading, scatters over a broad range. The dependence of critical fatigue parameters on ambient temperature and charging or discharging rate, along with the scattering nature of cycle-life is of practical significance. Through large-scale experimental investigations, it is shown how both temperatures and charging-discharging rates may influence critical parameters in the $C - N$ fatigue dependence for LIBs. The cycle-life N of a battery subject to an average charging rate C follows $C = c_0(T)N^{b(D)}$, where c_0 varies with temperature T and b is a function of the discharging rate D. It is further shown that the cycle-life of LIBs follows a lognormal distribution. The revealed cycle-life distribution of LIBs and their fatigue law enable the construction of a probabilistic $C - N$ model, which can be used to quantify the fatigue failure probability in LIBs. Results reported here are of compelling importance for the life-span evaluation and safety design of large-scale battery packing in electric vehicles and energy storage where tens of hundreds of batteries working in concert is desired.

1. Introduction

Fatigue is one of the most common causes accountings for the catastrophic failure in engineering systems with components subject to cyclic loads.[1] As a corollary, fatigue materials properties are of paramount significance for the design and safety-assessment of engineering structures. For repeatedly stressed solids, the well-known $S - N$ curve[2,3] is broadly adopted to characterize the dependence of their survival cycle number (N) on the stress magnitude (S). Such fatigue behavior is ubiquitously seen in engineer systems undergoing cyclic loading in broader sense, including mechanical, electric, magnetic, chemical, optical, etc. Lithium-ion batteries (LIBs), as a typical example, exhibit significant degradation when being charged and discharged under normal operating conditions. In contrast to stressed materials whose fatigue is well depicted by the $S - N$ curve, fatigue in LIBs involves intricate electro-chemo-thermo-mechanical-coupling processes,[4–6] and a physically sound correlation between cycle-life and battery loading conditions remains unclear. A variety of mechanisms, including evolution of electrode structure and active material,[7–9] thermal runaway,[10–12] gas generation,[12] solid-electrolyte interphase (SEI) formation,[13] interfacial contact and resistance change,[14] and so on, may collectively determines the cycle-life of batteries. The interwoven nature of all these aspects often obscures the full picture of fatigue processes.

Fatigue in LIBs is process-sensitive: variation in (dis)charging profiles and operating temperatures are known to be responsible for differences in cycle-life. Furthermore, when the same batch of batteries is tested under the same environmental conditions, their cycle-life scatters. Scattering cycle-life of LIBs further complicates lifetime prediction for LIBs, which is pivotal to engineering practice since batteries are often used in packs and modules. Scattering in the cycle-life of individual cells would certainly influence the collective performance of assembled battery packs and modules. The latter is of compelling need for the design, safety assessment, and recycling of, for example, traction batteries.

Many groups have put endeavors to explore methods to predict the cycle-life properties of LIBs. Both empirical models[15–17] and those based on degradation mechanisms[18–22] have been developed. In particular, the latter includes models based on variation in SEI thickness or resistance,[18,19] loss of active material,[20,21]

C. Chen, J. Wen, J. Liu, Y. Wei
State Key Laboratory of Nonlinear Mechanics
Institute of Mechanics
Chinese Academy of Sciences
Beijing 100190, China
E-mail: yujie_wei@lnm.imech.ac.cn
C. Chen, J. Wen, J. Liu, Y. Wei
School of Engineering Sciences
University of Chinese Academy of Sciences
Beijing 100049, China
Q. Zou
School of Applied Science
Beijing Information Science and Technology University
Beijing 100192, China
P. H. L. Notten
Eindhoven University of Technology
P.O. Box 513, MB Eindhoven 5600, The Netherlands
P. H. L. Notten
Forschungszentrum Jülich (IEK-9)
D-52425 Jülich, Germany
P. H. L. Notten
University of Technology Sydney
Broadway, Sydney, NSW 2007, Australia
Y. Wei
EIAS
Eastern Institute of Technology
Ningbo, Zhejiang 315200, China

The ORCID identification number(s) for the author(s) of this article can be found under https://doi.org/10.1002/aenm.202300942

DOI: 10.1002/aenm.202300942

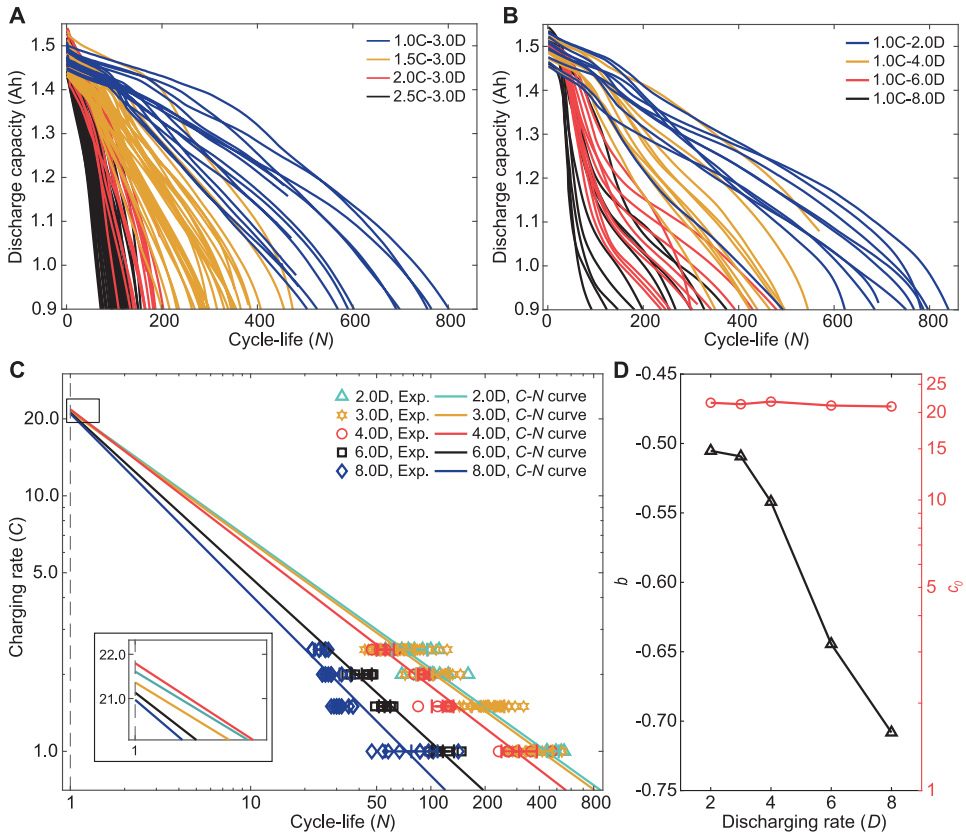

Figure 1. Impact of the charging and discharging rate on the $C-N$ curve. About 10 batteries were tested at each cycling condition (Table S1, Supporting Information). A) Discharge capacity versus cycle-life number plots of LFP batteries cycled with the same 3C discharging rate and different charging rates (1.0, 1.5, 2.0, and 2.5 C). B) The discharge capacity versus cycle-life number plots of LFP batteries cycled with the same charging rate (1 C) and different discharging rates (2.0, 3.0, 4.0, 6.0, and 8.0 C (denoted as D)). C) $C-N$ curves on a double-logarithmic scale at various fixed discharging rates and different charging rates. D) Slope b and the limiting charging rate c_0 versus discharging rate D of LISHEN LFP batteries, which were cycled at 25 °C.

and lithium plating.[22] Even machine-learning methods were adopted for cycle-life prediction of LIBs.[23–27] So far, the dependence of cycle-life on ambient temperature and (dis)charging rate, along with the scattering nature of cycle-life remains unknown. Through our experimental investigation, we will show the correlation of temperature and rate-dependence with the $C-N$ fatigue parameters for lithium-ion batteries. We also demonstrate that the cycle-life of LIBs follows a lognormal distribution. With both advances, we propose a probabilistic ($P-CN$) model for the cycle-life scattering assessment of LIBs, which supplies a statistic yet physically sound routine for safety analyses on LIBs.

2. Results and Discussion

2.1. $C-N$ fatigue in relation to (dis)charging

Commercial LFP ($LiFePO_4$)/graphite LIBs (LISHEN, 18650-type cylindrical battery, 1.5 Ah nominal capacity) were cycled at 25 °C under constant-current constant-voltage (CCCV) mode. Different C-rates were used during the constant-current (CC) charging and CC discharging stages, where 1C is equal to 1.5 A. In this paper, CC (dis)charging rates are used to differentiate the CCCV cycling conditions. For example, 1.0C–3.0D means the batteries are charged with 1.0C and discharged with 3.0C in CC stages during the CCCV cycling. The cut-off voltages in the constant-current (CC) charging stage and CC discharging stage are set to 4.0 and 2.0 V, respectively. The cut-off current during constant-voltage (CV) stage is set to 0.05C. Totally, 18 groups, 222 batteries were cycled for the LISHEN LFP batteries, and about 10 batteries were tested at each CCCV cycling condition. Detailed measurement settings and the cycled battery numbers for each cycling condition can be found in the Methods section and are summarized in the Table S1 (Supporting Information). **Figure 1**A and B display the influence of the CC charging and CC discharging rate on the maximum delivered discharging capacity evolution with cycling, respectively, in which different colors denote different CC (dis)charging C-rates used during the CCCV cycling. Note that discharging C-rates are abbreviated as D in all figures in what follows. Figure 1A shows the capacity curves of LFP batteries cycled with different CC charging rates (1.0, 1.5, 2.0 and 2.5C) but at the same 3.0C discharging rate. We see an accelerate fatigue rate with increased charging rate. Similarly, when being discharged with different discharging rates (2.0, 4.0, 6.0, and 8.0C (denoted as D)) but at the same CC charging rate of 1C, those discharged faster exhibit more pronounced capacity degradation and worse cycle-life performance (Figure 1B).

To quantify the impact of the CC (dis)charging rate on the cycle-life properties of batteries, we define the cycle-life (N) as

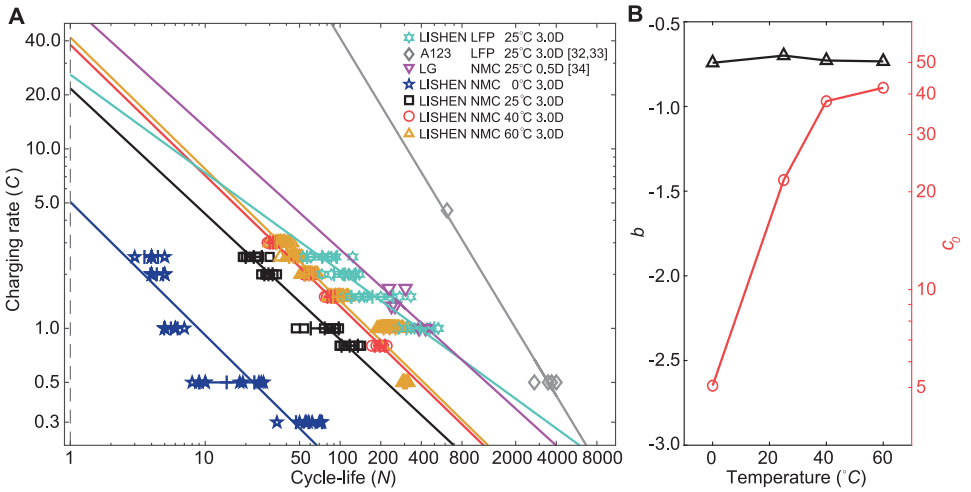

Figure 2. Temperature and material-dependent $C-N$ fatigue dependence. About 10 batteries were tested at each cycling condition (Table S2, Supporting Information). A) $C-N$ curves of various types of batteries cycled at fixed discharging rates but different temperatures. B) The slope b and intercept c_0 versus the temperature of the LISHEN NMC batteries, which are derived from the experimental data shown in (A).

the number of cycles until the delivered capacity of batteries falls below 80% of its nominal capacity, in line with the working protocol adopted by the electric vehicle batteries.[23,28–30] By plotting the charging rate (C) versus the cycle-life (N), we show in Figure 1C the influence of the charging rate profile. The following $C-N$ relationship holds

$$C = c_0 N^b \tag{1}$$

in which c_0 is the limiting charging rate, and b is a battery-related constant.[31] The limiting charging rate that causes battery failure during the first cycle (c_0 in Equation 2) shows, as expected, no relevance to the discharging rate. In contrast, b decreases as the discharging rate increases, which is also clearly indicated in Figure 1D. Now Equation 1 can also be expressed in the following form:

$$C = c_0 N^{b(D)} \tag{2}$$

where D is the discharge rate, and $b(D)$ is a discharging rate related function. According to Equation 2, an explicit expression to describe the effect of both charging (C) and discharging rate (D) on the cycle-life property can be represented as $\log N = \frac{\log C - \log c_0}{b(D)}$. The $C-N$ curve described in Equation 2 and shown in Figure 1 reveals the impact of the (dis)charging rate on the cycle-life performance at 25 °C. We will further explore how the temperature will influence the $C-N$ fatigue dependence in the following subsection.

2.2. Temperature and material sensitivity of the $C-N$ fatigue dependence

We evaluate the temperature and material effect on the $C-N$ fatigue dependence, using LISHEN NMC ($LiNi_xMn_yCo_{1-x-y}O_2$, LISHEN, 18650-type, nominal capacity of 2.6 Ah) and LFP LIBs. The NMC batteries are also cycled with CCCV mode with a cut-off current of 0.05C during CV stage. The cut-off voltages in the CC charging stage and CC discharging stage are set to 4.2 and 2.75 V, respectively. 19 groups and 341 LISHEN NMC batteries were cycled with CCCV mode. The (dis)charging parameters and battery number of these LISHEN NMC LIBs are detailed in the Table S2 (Supporting Information). The cycle-life data of other manufacturers' batteries from other papers, given in Table S3 (Supporting Information), are also analyzed with the $C-N$ fatigue dependence. **Figure 2**A shows the charging C-rate versus the cycle-life N curves of different-type LIBs with several CC (dis)charging rates at various temperatures. It is evidently seen that all batteries follow the $C-N$ dependence upon cycling. For the cycled NMC batteries from the same batch, we adopted different CC charging rates but the same 3.0C discharging rate during the CCCV cycling at different temperatures. The fitted linear $C-N$ plots of the NMC batteries at various temperatures (0, 25, 40, and 60 °C) are nearly parallel, and the slope of the linear $C-N$ expression, characterized by b, is unchanged for theses batteries (Figure 2B). This may imply that b is irrelevant to the ambient temperature. The limiting charging rate, namely the intercept c_0 in Equation 2, decreases as the temperature decreases, which is also clearly indicated in Figure 2B. Therefore, we may rewrite Equation 2 in a more precise form as:

$$C = c_0\,(T)\,N^{b(D)} \tag{3}$$

where $c_0(T)$ varies with temperature T.

Further comparing the fitted linear $C-N$ plots of the LISHEN NMC (black line in Figure 2A) and LISHEN LFP (turquoise line in Figure 2A) batteries, we can see that the parameter c_0 and b are different between distinct battery types, albeit they were cycled with corresponding 3.0C discharging rate in CCCV cycling at 25 °C. This indicates that the electrode materials will influence the power parameters in the $C-N$ law of LIBs. Furthermore, we observe a significant difference in cycle-life performance compared with LIBs with the same LFP electrode materials but different manufacturers, e.g. data using LISHEN (turquoise line in

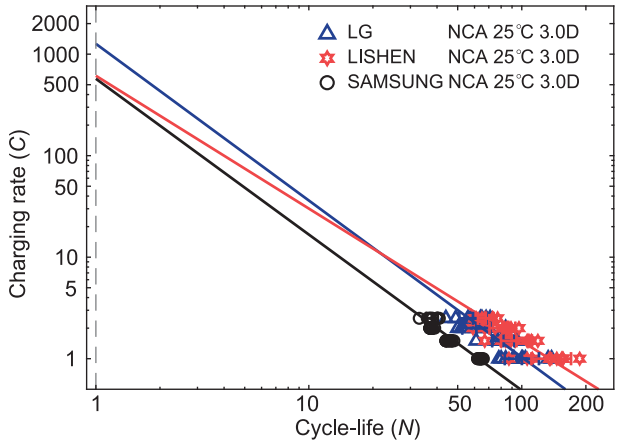

Figure 3. $C-N$ fatigue dependence for filtering out better batteries. 10 batteries were tested at each cycling condition (Table S4, Supporting Information). $C-N$ curves of the LG, LISHEN, and SAMSUNG 18650-type NCA batteries cycled at the fixed discharging rates (3.0 D) and different charging rates at 25 °C. The tested 18650-type NCA batteries are all with the same nominal capacity of 3.35 Ah.

Figure 2A) and those with A123 (grey line in Figure 2A, nominal capacity of 1.1 Ah) batteries at 25 °C.[32,33] This deviation is also visible between the LISHEN (black line in Figure 2A) and LG (magenta line in Figure 2A, nominal capacity of 3.0 Ah) 18 650 NMC type batteries.[34] Such a difference can be quantified by using the $C-N$ model (Equation 3). It is worth to note that the batteries used in Figure 2A are with different nominal capacities. We further tested three manufacturers' (LG, LISHEN, and SAMSUNG) 18650-type $LiNi_xCo_yAl_{1-x-y}O_2$ (NCA) batteries with the same nominal capacity of 3.35 Ah. **Figure 3** shows the $C-N$ fatigue of these batteries (LG, LISHEN, and SAMSUNG 18650-type, NCA). These three kinds of batteries have different $C-N$ dependence performance albeit with the same battery materials, nominal capacity, and test temperatures. Therefore, as broadly seen that materials from different suppliers may have distinct properties, the power performance of batteries relies on their design parameters, material selections, applied processing, and so on. Those dependence of different origins in collection are characterized by c_0 and b in Equation 3. For batteries of the same type and same nominal capacity, those with lower negative value of b point to poorer cycle-life properties, and greater c_0 means better performance.

The significant difference in battery cycle-life of the same batch is an important feature in most rechargeable batteries,[32–34] which is evidently seen from the significantly scattering cycle-life curves shown in Figures 1–3 under the same (dis)charging mode and temperature. Such cycle-life scattering behavior may be caused by the divergence of manufacturing, dynamic operating protocols, in-use, or storage conditions, etc. Depicting the random cycle-life performance is important to the evaluation of cell consistency in cycle-life property, and large-scale battery packing applications in electric vehicles and energy storage. In the following section, we determine the cycle-life distribution and elaborate on the developed probabilistic $C-N$ model for evaluating the fatigue failure probability in LIBs.

2.3. Probabilistic $C-N$ curves evaluating cycle-life property scattering

For given fatigue datasets, invalid distribution models can lead to inaccurate or biased estimates of lifetime quantiles in tail, causing immeasurable personal and property loss.[35,36] To determine the appropriate cycle-life distribution in LIBs, a total number of 100 LISHEN NMC batteries are cycled in the 1.0C–3.0D mode at 60 °C (see Table S2, Supporting Information) and a comparative analysis from several perspectives is further considered (**Figure 4**). Figure 4A shows graphical frequency histogram distributions of N. The cycle-life distribution is asymmetric with a longer tail at the right. Since Lognormal[37] and Weibull distributions[38] are the most commonly employed distributions for lifetime and fatigue analyses,[34,39] we estimate the probability density curves of these two distributions by using the cycle-life frequency data. The curve derived from the Lognormal distribution is slightly right-skewed and has a longer right-tail. In contrast, the Weibull distribution is slightly left-skewed with a longer left-tail (Figure 4A). Figure 4B shows the quantile-quantile plots (QQ-plots, the detailed description is shown in the Methods section)[40] of Lognormal distribution and Weibull distribution. The shadowed regions in the QQ-plots are the 95% pointwise confidence bands based on the Lognormal and Weibull confidence interval. In contrast to the Weibull QQ-plot (see the inset of Figure 4B), all the sample quantiles fall within the 95% pointwise confidence bands in the Lognormal QQ-plot (Figure 4B), implying Lognormal distribution being more appropriate for the cycle-life data of LIBs.

We further use cumulative-distribution-function (CDF) analyses to sift the proper one from those distributions to depict the cycle-life of LIBs. Figure 4C shows the Kaplan-Meier estimate of the CDF, i.e., the empirical CDF and its 95% confidence bounds for the CDF using Greenwood's formula.[41,42] The CDF estimation reliability displayed in Figure 4D suggests CDF of Lognormal distribution is agree well with the empirical CDF. The Weibull distribution is conservative at high reliability regions, while a bit aggressive at low reliabilities. Different statistical investigations suggest that the lognormal distribution is better suited for the cycle-life property analyses in LIBs.

As demonstrated in Figure 4, the cycle-life of the same batch of LIBs, cycled at the same (dis)charging conditions, exhibits a wide-range distribution. The scattering of fatigue life commonly decreases with the increased loading levels.[43] It hence brings up the need for probabilistic $C-N$ ($P-CN$) model for the cycle-life scattering assessment in LIBs, as have done for probabilistic $S-N$ analysis for stressed materials. **Figure 5**A shows the scatter of cycle-life from different charging rates of the applied LISHEN NMC batteries. Apart from the 1.0C–3.0D tests 100 batteries, each other condition (1.5C-, 2.0C-, 2.5C-, and 3.0C-3.0D) tests 30 batteries during cycling. As expected, the scatter band of cycle-life of LIBs decreases with the increasing charging rate. For the log-cycle-life curves of the LIBs cycled with different charging rates shown in the inset of Figure 5A, the variance seems to be homogeneous. To further determine whether the variances of log-cycle-life between serval charging rates are equal, we applied Bartlett's Test[44] based on a chi-square statistic. The obtained Bartlett's chi-square value is 7.25, and the p-value is 0.12,

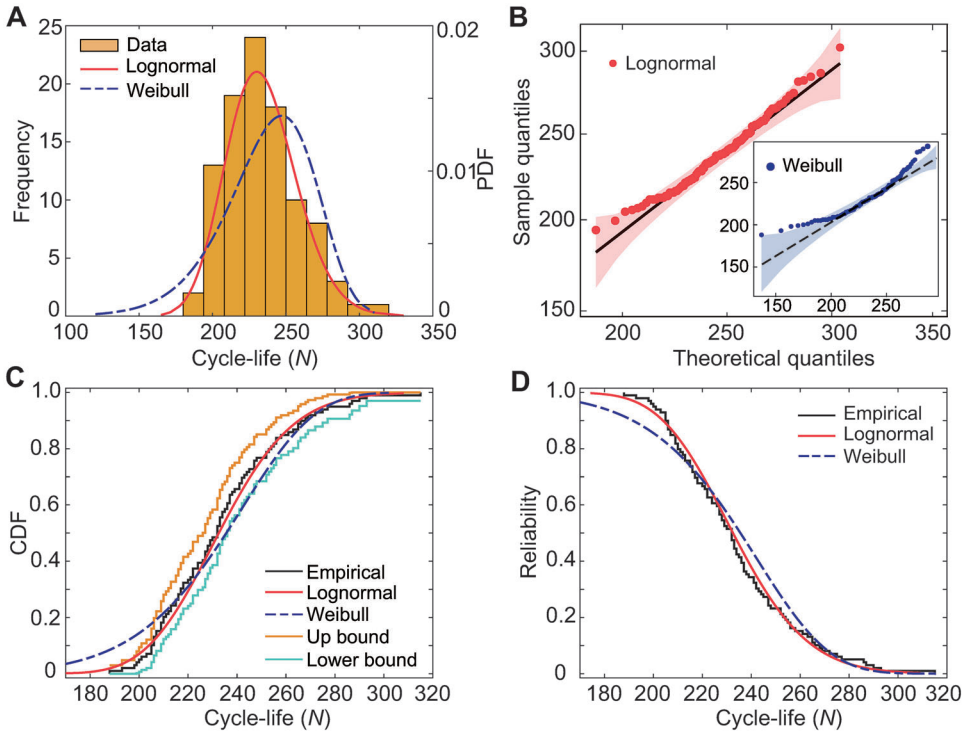

Figure 4. Comparison between the Lognormal and Weibull distribution on cycle-life analyses of LIBs. A) Frequency histogram with the fitted probability density function (PDF). B) Lognormal QQ-plot with inset showing the Weibull QQ-plot. C) Cumulative empirical CDF distribution, and D) reliability estimation of both the Lognormal and Weibull distributions.

implying that we cannot reject the homogeneous variance with sufficient evidence.

The derivation details of the $P-CN$ model is described in the Methods section. Figure 5B and C show the predicted $P-CN$ curve from Equations (7) and (8), respectively. To better reveal the predictability in the tail regions, we display in Figure 5B the $P-CN$ curves of cycle-life. Corresponding log-log plots are also supplied in Figure S1A (Supporting Information). The median $C-N$ curve (blue line in Figure 5B; Figure S1A, Supporting Information) gives the 50% failure $P-CN$ curve. The black and red dotted lines in Figure 5B are the 5% and 1% failure $P-CN$ curves, respectively. When fatigue failure data are limited, the estimation of probabilistic $P-CN$ curve becomes uncertain.[45] It is necessary to establish the lower bound of the fatigue life at a given failure probability p. Figure 5C shows the estimated 1% failure $P-CN$ curve with 95% confidence in log-log coordinate, a counter plot of cycle-life is also available in Figure S1B (Supporting Information). The cycle-life of LISHEN LFP batteries were also demonstrated to follow the lognormal distribution (Figure S2, Supporting Information). Corresponding $P-CN$ curves are shown in Figure S3 (Supporting Information). With the proposed $P-CN$ model, the fatigue failure probability of LIBs can be well quantified.

3. Conclusions

In this work, we revealed the impact of temperature and (dis)charging rate on the cycle-life properties of LIBs. Through the development of the $C-N$ fatigue dependence for LIBs, our experimental data suggest that larger discharging rates lead to faster cycle-life degradation, which can be quantified by the slope b of the log-log plot of the cycle-life number N versus charging rate C. Since the cycle-life number N will reduce with cycling, the slope b is negative in the log-log plot of $C-N$ curve: faster discharging rate leads to quicker reduction in cycle-life numbers, and hence greater magnitude of b. In parallel, we decipher the effect of temperature upon cycle-life properties of batteries. It is found that the power b of the $C-N$ curve is insensitive to variation in temperature. The limiting charging rate c_0, in contrast, shows strong dependence on ambient temperature. In combination, we find the cycle-life number N of a battery subject to an average charging rate C may be further refined as $C = c_0\,(T)N^{b(D)}$, where c_0 varies with temperature T and b is a function of the discharging rate D.

The physical significance of the coefficient and the exponent parameters in $C-N$ fatigue law (b and c_0) lies in that: 1) one may use them to quantify the cyclic performance of batteries; 2) These parameters offer a guidance to customers for selecting appropriate battery types, as manifested in Figure 2A and Figure 3; 3) the manufacturers may use it to identify the performance of active materials as well as the consistence of manufacturing process.

It is further revealed that the cycle-life of batteries scatters (see Figure 4) even for the same batch that is subjected to the same operational conditions. Like cycle-life scattering of other solids under external loading, this scattering phenomenon is inherent to the cycle-life of batteries due to the divergence of manufacturing processing and dynamic operation. Based on different statistical investigations, we reveal that the lognormal distribution is the

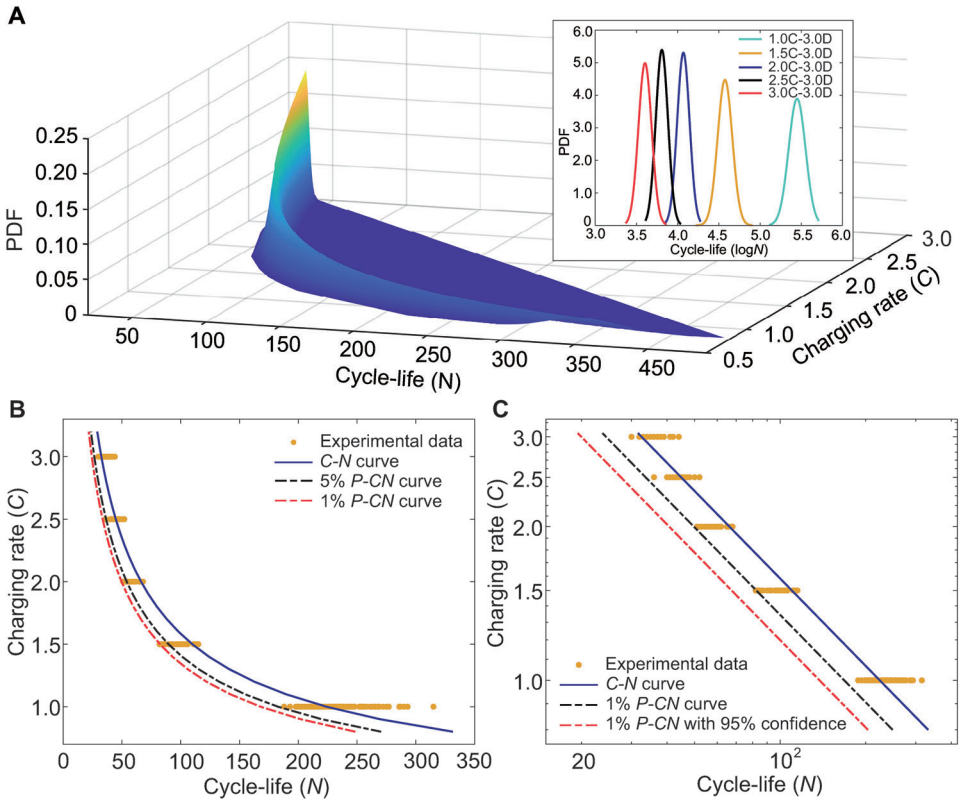

Figure 5. *P − CN* curves for the fatigue failure probability of LIBs. A) The scatter of cycle-life of the LISHEN NMC batteries cycled with different charging rates, with inset showing the corresponding Logarithm curves. B) The *P − CN* curves of cycle-life. C) The lower tolerance limit *P − CN* curves of log-cycle-life.

appropriate model for cycle-life scattering analyses of LIBs. The revealed cycle-life equation and the distribution of LIBs' cycle-life enable us to construct a probabilistic *C − N* model to evaluate the fatigue failure probability in LIBs.

As indicated, the demonstrated *C − N* dependence in LIBs resembles very much with the *S − N* fatigue in materials while cyclic using. Nevertheless, we would like to note that the degradation mechanisms of both systems are of significant difference. It is well known that the crack initiations and propagations are the main reason causing the *S − N* fatigue behavior in materials in repeated mechanical use. Although both the cathode and anode materials experience prominent iterative volume expansion/shrink, along with the cyclic tensile/compressive stress during electrochemical cycling,[5,46,47] complex electro-chemo-thermo-mechanical-coupling factors are driving the degradation of LIBs. We assume that the *C − N* fatigue in LIBs might be a mechanical-dominant phenomenon. However, it remains challenging to quantify the mechanical-induced contribution to the degradation. We believe this work will open further investigations toward LIBs' *C − N* fatigue in unveiling the underlying mechanisms, both from theoretical and experimental perspectives. Results reported here are of compelling need for the life-span evaluation and safety design of tract batteries that involve the function of tens of hundreds of batteries working in concert, where both deterministic physical laws and statistical nature of cycle-life are the intrinsic nature of such engineering system.

4. Experimental Section

Battery Cycling: Commercial LFP($LiFePO_4$)/graphite batteries (LISHEN, 18 650 cylindrical battery, 1.5 Ah nominal capacity), NMC/graphite batteries (LISHEN, 18 650 cylindrical battery, 2.6 Ah nominal capacity), and NCA/graphite batteries (LG, LISHEN, and Samsung, 18 650 cylindrical battery, 3.35 Ah nominal capacity) were cycled by using the NEWARE battery testing systems. The sampling frequency was set to 1 Hz. Temperature control was realized in an environmental chamber. Typical constant-current constant-voltage (CCCV) charging and discharging profiles for the cycling measurements were employed. For the LFP batteries, the cut-off voltages in the constant-current (CC) charging stage and CC discharging stage are set to 4.0 and 2.0 V, respectively. For NMC batteries, the higher and lower cut-off voltages are 4.2 and 2.75 V, respectively, while those for NCA batteries are 4.2 and 2.65 V, respectively. The cut-off current during constant-voltage (CV) stage is set to 0.05C. Noting that 1C is equal to 1.5, 2.6, and 3.35 A for the LISHEN-LFP, LISHEN-NMC, and NCA batteries, respectively. The dataset includes 49 groups and 683 batteries in total, and each group were applied with the same CC charging and CC discharging rate profile. The details about the 49 charging-discharging profiles are listed in detail in Tables S1, S2, and S4 (Supporting Information). Cycling data of the 683 LIBs can be found in uploaded source data. The cycle-life data of batteries from literatures used in Figure 2A were given in Table S3 (Supporting Information).

Quantile-Quantile Plots: The quantile-quantile plot (QQ plot) evaluates whether sample observations come from a specified distribution.[40] It compares two distributions through matching a common set of quantiles by displaying the quantiles of the sample data versus theoretical quantile values from the distribution. Specifically, for a random variable *y* and a sample dataset$\{y_1,\cdots, y_n\}$. The sample data values are first

ordered from the smallest to the largest, denoting as $\{y_{(1)},\cdots, y_{(n)}\}$, where $y_{(i)}$ was the i-th ordered value. Then n sample quantiles are given as $F_n(y_{(i)}) = \frac{i-0.5}{n}$, $i = 1, 2, \ldots, n$. The QQ plot was given by a scatterplot of the sample quantiles, $y_{(i)}$, against the corresponding quantiles from the theoretical distribution, $F^{-1}(F_n(y_{(i)}))$, where $F(\cdot)$ was the theoretical distribution function and $P(y \le F^{-1}(p)) = p$. The sample quantile values appear along the y-axis, and the theoretical values of the specified distribution at the same quantiles appear along the x-axis; when the sample data comes from the specified distribution, the points fall on a line.

P − CN Model Derivation: The logarithm of cycle-life, N, of batteries at a given charging rate C, can be expressed as the normal distribution:

$$F(X) = P(x \le X) = \frac{1}{\sqrt{2\pi}\sigma}\int_{-\infty}^{X} \exp\left[-\frac{1}{2}\left(\frac{x-\mu}{\sigma}\right)^2\right] dx \tag{4}$$

where $x = \log N$, μ and σ were respectively the mean and the standard deviation of x. Equation (4) gives the cumulative probability of failure for x, that was the proportion of the population falling at lives no longer than X.

The mean $C - N$ curve can be obtained by using the maximum likelihood method. Let $\hat{\mu}$ denote the estimate of μ (the mean $C - N$ for the population), which was written as:

$$\hat{\mu} = \frac{\bar{y} - \hat{a}}{\hat{b}}, \text{with } \hat{b} = \frac{\sum_{i=1}^{n}(x_i - \bar{x})(y_i - \bar{y})}{\sum_{i=1}^{n}(x_i - \bar{x})^2} \text{ and } \hat{a} = \bar{y} - \hat{b}\bar{x} \tag{5}$$

where $\hat{a}$ was the estimate of a, $a = \ln c_0$ (c_0 the limiting charging rate), $\hat{b}$ was the estimate of slope parameter b in $C - N$ curve (Equations 1–3). $\bar{x} = \frac{1}{n}\sum_{i=1}^{n} x_i$, $y_i = \ln C_i$, $\bar{y} = \frac{1}{n}\sum_{i=1}^{n} y_i$, and n was the size of the dataset.

The standard deviation $\hat{\sigma}$ of the logarithm of the cycle-life from the mean $C - N$ curve for the given population is:

$$\hat{\sigma} = \sqrt{\frac{\sum_{i=1}^{n}(x_i - \hat{x}_i)^2}{n-q}} \tag{6}$$

where q was the number of parameters estimated in the model and $q = 2$ here. The $P - CN$ curve corresponding to a certain probability failure p was:

$$x_{(p)} = \hat{\mu} + z_p\hat{\sigma} \tag{7}$$

where z_p was the p quantile of the standard normal distribution function, i.e., $\Phi(z_p) = p$, and $\Phi(\cdot)$ was the cumulative probability distribution function of the standard normal distribution.

In practical exercise, it was needed to assess the proportion of data that lies above a lower limit, so that p-percent of measurements will not fall below the lower limit. The corresponding lower tolerance limits based on computations from a series of measurements $x_1, x_2, \cdots, x_n$ was defined. The estimated lower limit of the cycle-life at a given probability of failure, at the confidence level $1 - \alpha$, was in the form of:

$$\hat{x}_{(p,1-\alpha)} = \hat{\mu} + k(p, 1-\alpha, \nu)\,\hat{\sigma} \tag{8}$$

where, $k(p, 1-\alpha, \nu)$ was the one-sided tolerance limit for a normal distribution, which can be calculated directly from the following set of formulas[48]

$$k(p, 1-\alpha, \nu) = \frac{z_p - z_\alpha\sqrt{\frac{1}{n}\left[1 - \frac{z_\alpha^2}{2(n-1)}\right] + \frac{z_p^2}{2(n-1)}}}{1 - \frac{z_\alpha^2}{2(n-1)}} \tag{9}$$

For a given set of data, Equations (7) to (9) were used to obtain the information it was shown in Figure 4. To sum up, the specific implement steps as follows:

Step 1: Obtain the cycle-life data of n batteries, $\{C_i, N_i\}, i = 1, 2, \cdots, n$, and adopt the logarithm transformation, $x_i = \ln N_i$, $y_i = \ln C_i$.

Step 2: According to $C - N$ model $C_i = c_0 N_i^b$ and the life of battery follows Lognormal distribution, i.e., $\ln N_i = \frac{1}{b}\ln C_i - \frac{\ln c_0}{b} + \varepsilon$, $\varepsilon \sim N(\frac{1}{b}\log C_i - \frac{\ln c_0}{b}, \sigma^2)$, the estimate of parameters can be obtained. The specific estimators were shown in Equations (5) and (6).

Step 3: Any p quantile of log cycle-life at charging rate C can be obtained based on Equation (7).

Step 4: *The* lower tolerance limits can be obtained according to Equations (8) and (9).

Supporting Information

Supporting Information is available from the Wiley Online Library or from the author.

Acknowledgements

C.C., Q.Z. contributed equally to this work. The authors acknowledge support from the National Natural Science Foundation of China (NSFC) Basic Science Center for 'Multiscale Problems in Nonlinear Mechanics' (No. 11988102). C.C. acknowledges support from the Chinese Academy of Sciences (No. E1Z1010901). Q.Z. acknowledges support from R&D Program of Beijing Municipal Education Commission (KM202311232008). J.W. acknowledges support from NSFC (No. 12002343).

Conflict of Interest

The authors declare no conflict of interest.

Author Contributions

Y.W. conceived the project. C.C. and Y.W. designed the experiments, C.C. and J.L. performed the experiments and the $C - N$ data analyses, Q.Z. and J.W. developed the statistical $P - CN$ analyses. Y.W., C.C., Q.Z., J.W. and P.N. wrote the paper. All authors analyzed data, discussed the results, reviewed, and edited the manuscript.

Data Availability Statement

The data that support the findings of this study are openly available in Science Data Bank at https://doi.org/10.57760/sciencedb.07456, reference number 7456.

Keywords

$C - N$ fatigue, cycle-life distribution, (dis)charging rate, probabilistic fatigue, temperature effect

Received: March 28, 2023
Revised: May 10, 2023
Published online: May 26, 2023

[1] S. Suresh, *Fatigue of Materials*, 2nd edn, Cambridge Uni. Press, **1998**.
[2] A. Wöhler, *Zeitschrift für Bauwesen* **1860**, *10*, 160.
[3] O. H. Basquin, *Proc., Am. Soc. Test. Mater.* **1910**, *10*, 625.

[4] R. Deshpande, M. Verbrugge, Y. T. Cheng, J. Wang, P. Liu, *J. Electrochem. Soc.* **2012**, *159*, A1730.
[5] M. Ebner, F. Marone, M. Stampanoni, V. Wood, *Science* **2013**, *342*, 716.
[6] C. Chen, M. Jiang, T. Zhou, L. Raijmakers, E. Vezhlev, B. Wu, T. Schulli, D. Danilov, Y. Wei, R. Eichel, *Adv. Energy Mater.* **2021**, *11*, 2003939.
[7] Y. Chen, Z. Wang, X. Li, X. Yao, C. Wang, Y. Li, W. Xue, D. Yu, S. Kim, F. Yang, A. Kushima, G. Zhang, H. Huang, N. Wu, Y. Mai, J. B. Goodenough, *Nature* **2020**, *578*, 251.
[8] M. G. Boebinger, D. Yeh, M. Xu, B. Miles, B. Wang, M. Papakyriakou, J. Lewis, N. Kondekar, F. Cortes, S. Hwang, X. Sang, D. Su, R. Unocic, S. Xia, T. Zhu, M. McDowell, *Joule* **2018**, *2*, 1783.
[9] J. Wen, Y. Wei, Y. T. Cheng, *J Mech Phys Solids* **2018**, *116*, 403.
[10] A. Kvasha, C. Gutierrez, U. Osa, I. de Meatza, J. Blazquez, H. Macicior, I. Urdampilleta, *Energy* **2018**, *159*, 547.
[11] T. Yokoshima, D. Mukoyama, F. Maeda, T. Osaka, K. Takazawa, S. Egusa, S. Naoi, S. Ishikura, K. Yamamoto, *J. Power Sources* **2018**, *393*, 67.
[12] D. P. Finegan, M. Scheel, J. B. Robinson, B. Tjaden, I. Hunt, T. J. Mason, J. Millichamp, M. Di Michiel, G. J. Offer, G. Hinds, *Nat. Commun.* **2015**, *6*, 6924.
[13] M. B. Pinson, M. Z. Bazant, *J. Electrochem. Soc.* **2012**, *160*, A243.
[14] J. Christensen, J. Newman, *J. Electrochem. Soc.* **2004**, *151*, A1977.
[15] J. Wen, Q. Zou, C. Chen, Y. Wei, *Electrochim. Acta* **2022**, *434*, 141300.
[16] E. V. Thomas, I. Bloom, J. P. Christophersen, V. S. Battaglia, *J. Power Sources* **2008**, *184*, 312.
[17] I. Bloom, B. W. Cole, J. J. Sohn, S. A. Jones, E. G. Polzin, V. S. Battaglia, G. L. Henriksen, C. Motloch, R. Richardson, T. Unkelhaeuser, D. Ingersoll, H. L. Case, *J. Power Sources* **2001**, *101*, 238.
[18] M. Safari, M. Morcrette, A. Teyssot, C. Delacourt, *J. Electrochem. Soc.* **2009**, *156*, A145.
[19] D. Li, D. L. Danilov, B. Zwikirsch, M. Fichtner, Y. Yang, R. A. Eichel, P. H. L. Notten, *J. Power Sources* **2018**, *375*, 106.
[20] J. Wang, P. Liu, J. Hicks-Garner, E. Sherman, S. Soukiazian, M. Verbrugge, H. Tataria, J. Musser, P. Finamore, *J. Power Sources* **2011**, *196*, 3942.
[21] Y. Ye, Y. Shi, A. A. O. Tay, *J. Power Sources* **2012**, *217*, 509.
[22] X.-G. Yang, Y. Leng, G. Zhang, S. Ge, C.-Y. Wang, *J. Power Sources* **2017**, *360*, 28.
[23] K. A. Severson, P. M. Attia, N. Jin, N. Perkins, B. Jiang, Z. Yang, M. H. Chen, M. Aykol, P. K. Herring, D. Fraggedakis, *Nat. Energy* **2019**, *4*, 383.
[24] P. M. Attia, A. Grover, N. Jin, K. A. Severson, T. M. Markov, Y. H. Liao, M. H. Chen, B. Cheong, N. Perkins, Z. Yang, P. K. Herring, M. Aykol, S. J. Harris, R. D. Braatz, S. Ermon, W. C. Chueh, *Nature* **2020**, *578*, 397.
[25] Z. Tong, J. Miao, S. Tong, Y. Lu, *J Clean Prod* **2021**, *317*, 128265.
[26] X. Hu, L. Xu, X. Lin, M. Pecht, *Joule* **2020**, *4*, 310.
[27] C. Lin, H. Mu, R. Xiong, W. Shen, *Appl. Energy* **2016**, *166*, 76.
[28] J. Shen, S. Dusmez, A. Khaligh, *IEEE Trans Industr Inform* **2014**, *10*, 2112.
[29] X. Han, M. Ouyang, L. Lu, J. Li, *J. Power Sources* **2014**, *268*, 658.
[30] M. H. S. M. Haram, J. W. Lee, G. Ramasamy, E. E. Ngu, S. P. Thiagarajah, Y. H. Lee, *Alex. Eng. J.* **2021**, *60*, 4517.
[31] J. Wen, Q. Zou, Z. Zhang, J. Shi, Y. Wei, *Acta Mech. Sin.* **2022**, *38*, 222108.
[32] Y. Preger, H. M. Barkholtz, A. Fresquez, D. L. Campbell, B. W. Juba, J. Roman-Kustas, S. R. Ferreira, B. Chalamala, *J. Electrochem. Soc.* **2020**, *167*, 120532.
[33] P. Keil, A. Jossen, *J. Energy Storage* **2016**, *6*, 125.
[34] R. Mathieu, O. Briat, P. Gyan, J.-M. Vinassa, *Appl. Energy* **2021**, *283*, 116344.
[35] F. G. Pascual, G. Montepiedra, *IEEE Trans. Reliab.* **2005**, *54*, 43.
[36] Q. Zou, J. Zhao, J. Wen, *Int. J. Fatigue* **2022**, *167*, 107326.
[37] M. V. Ratnaparkhi, W. J. Park, *IEEE Trans. Reliab.* **1986**, *35*, 312.
[38] W. Weibull, *Handlingar* **1939**, *151*, 1.
[39] J. S. Kim, B.-J. Yum, *Comput. Stat. Data Anal.* **2008**, *53*, 477.
[40] M. B. Wilk, R. Gnanadesikan, *Biometrika* **1968**, *55*, 1.
[41] D. R. Cox, D. Oakes, *Analysis of Survival Data* Chapman & Hall, **1984**.
[42] J. F. Lawless, *Statistical Models and Methods for Lifetime Data*, 2nd ed. Wiley, **2003**.
[43] C. Li, S. Wu, J. Zhang, L. Xie, Y. Zhang, *Int. J. Fatigue* **2020**, *139*, 105789.
[44] M. S. Bartlett, *Proc. R. Soc. Lond. B. Biol. Sci.* **1937**, *160*, 268.
[45] K. O. Ronold, I. Lotsberg, *Mar. Corros. Offshore Struct., Pap. Symp.* **2012**, *27*, 29.
[46] J. Ma, J. Sung, Y. Lee, Y. Son, S. Chae, N. Kim, S.-H. Choi, J. Cho, *Adv. Energy Mater.* **2020**, *10*, 1903400.
[47] C. R. Hernandez, A. Etiemble, T. Douillard, D. Mazouzi, Z. Karkar, E. Maire, D. Guyomard, B. Lestriez, L.l Roué, *Adv. Energy Mater.* **2018**, *8*, 1701787.
[48] M. G. Natrella, *Experimental Statistics. National Bureau of Standards Handbook 91* US Department of Commerce, **1963**.